

AWARD NUMBER: W81XWH-15-1-0372

TITLE: Discovery of Novel N-Nicotinamide Methyltransferase Inhibitors to Combat Obesity-Linked Osteoarthritis and Metabolic Disease Among Veterans and Beneficiaries

PRINCIPAL INVESTIGATOR: Watowich, Stanley J.

CONTRACTING ORGANIZATION: University of Texas Medical Branch at Galveston
Galveston, TX 77555

REPORT DATE: October 2016

TYPE OF REPORT: Annual

PREPARED FOR: U.S. Army Medical Research and Materiel Command
Fort Detrick, Maryland 21702-5012

DISTRIBUTION STATEMENT: Approved for Public Release;
Distribution Unlimited

The views, opinions and/or findings contained in this report are those of the author(s) and should not be construed as an official Department of the Army position, policy or decision unless so designated by other documentation.

REPORT DOCUMENTATION PAGE				Form Approved OMB No. 0704-0188	
Public reporting burden for this collection of information is estimated to average 1 hour per response, including the time for reviewing instructions, searching existing data sources, gathering and maintaining the data needed, and completing and reviewing this collection of information. Send comments regarding this burden estimate or any other aspect of this collection of information, including suggestions for reducing this burden to Department of Defense, Washington Headquarters Services, Directorate for Information Operations and Reports (0704-0188), 1215 Jefferson Davis Highway, Suite 1204, Arlington, VA 22202-4302. Respondents should be aware that notwithstanding any other provision of law, no person shall be subject to any penalty for failing to comply with a collection of information if it does not display a currently valid OMB control number. PLEASE DO NOT RETURN YOUR FORM TO THE ABOVE ADDRESS.					
1. REPORT DATE October 2016		2. REPORT TYPE Annual		3. DATES COVERED 30 Sep 2015 - 29 Sep 2016	
4. TITLE AND SUBTITLE Discovery of Novel N-Nicotinamide Methyltransferase Inhibitors to Combat Obesity-Linked Osteoarthritis and Metabolic Disease Among Veterans and Beneficiaries				5a. CONTRACT NUMBER	
				5b. GRANT NUMBER W81XWH-15-1-0372	
				5c. PROGRAM ELEMENT NUMBER	
6. AUTHOR(S) Stanley J. Watowich E-Mail: watowich@xray.utmb.edu				5d. PROJECT NUMBER	
				5e. TASK NUMBER	
				5f. WORK UNIT NUMBER	
7. PERFORMING ORGANIZATION NAME(S) AND ADDRESS(ES) AND ADDRESS(ES) University of Texas Medical Branch 301 UNIVERSITY BLVD GALVESTON TX 77555-5302				8. PERFORMING ORGANIZATION REPORT NUMBER	
9. SPONSORING / MONITORING AGENCY NAME(S) AND ADDRESS(ES) U.S. Army Medical Research and Materiel Command Fort Detrick, Maryland 21702-5012				10. SPONSOR/MONITOR'S ACRONYM(S)	
				11. SPONSOR/MONITOR'S REPORT NUMBER(S)	
12. DISTRIBUTION / AVAILABILITY STATEMENT Approved for Public Release; Distribution Unlimited					
13. SUPPLEMENTARY NOTES					
14. ABSTRACT Nicotinamide N-methyltransferase (NNMT) has been implicated in osteoarthritis, metabolic disorders, cardiovascular disease, cancer, kidney disease, and Parkinson's disease that impact the military, their dependents, and the general population. This project is developing drug candidates that specifically target NNMT and produce targeted reductions in white adipose tissue, leading to significant weight loss and improvements in obesity-linked comorbidities. Towards this end, we developed the first assay to directly monitor NNMT product formation and activity in real-time, resulting in the enhanced capacity to collect accurate NNMT kinetic data. Detailed kinetic data analysis has resulted in the detailed molecular characterization of NNMT reaction mechanism, and, importantly, discovery of novel drug-like nanomolar NNMT inhibitors. These drug candidates showed attractive cellular permeability flux when tested in membrane transport assays. Synthesis scale-up of the most promising drug candidates has been achieved. Proof-of-concept evaluation in mouse models of diet-induced obesity is awaiting final IACUC approval, but is anticipated to commence within the month.					
15. SUBJECT TERMS metabolic disease; obesity; osteoarthritis; drug candidates					
16. SECURITY CLASSIFICATION OF:			17. LIMITATION OF ABSTRACT Unclassified	18. NUMBER OF PAGES 57	19a. NAME OF RESPONSIBLE PERSON USAMRMC
a. REPORT Unclassified	b. ABSTRACT Unclassified	c. THIS PAGE Unclassified			19b. TELEPHONE NUMBER (include area code)

Table of Contents

	<u>Page</u>
1. Introduction.....	4
2. Keywords.....	5
3. Accomplishments.....	6
4. Impact.....	14
5. Changes/Problems.....	15
6. Products.....	16
7. Participants & Other Collaborating Organizations.....	18
8. Special Reporting Requirements.....	20
9. Appendices.....	21

1. Introduction

Our project aligned with FY14 PRMRP Topic Areas metabolic disease (including obesity, obesity-associated metabolic disease, and type 2 diabetes) and osteoarthritis. Das et al. reported that over one-third of US veterans and their post-adolescent dependents were clinically obese, making obesity and obesity-linked comorbidities one of the top health issues faced by the DoD healthcare system. Treating obesity-linked chronic diseases currently accounts for ~10% of veteran's healthcare expenditures. Unfortunately, the vast majority of efforts to reduce obesity through diet, exercise, and/or appetite suppression have not had long-term success, and bariatric surgery carries many risks including death. In this project, we propose a radical rethinking of this problem to move away from failed efforts to reduce calorie input relative to calorie expenditure in the hope that body fat (white adipose tissue) and excess body mass will decrease. Instead, we are developing and testing novel small molecule drugs that are predicted to directly increase white adipose tissue energy expenditures, thus reducing body fat and total body mass. To achieve this anti-obesity drug breakthrough, our project exploits recent observations that down-regulation of the enzyme nicotinamide N-methyltransferase (NNMT) could shrink white adipose tissue and produce significant weight loss in animal models, without the necessity of reducing calorie intake. To validate the in vitro activity of novel NNMT inhibitors, we developed the first assay capable of directly monitoring NNMT product formation and activity in real-time, resulting in the enhanced capacity to collect accurate NNMT kinetic data. Using this assay, and accessory tests, we have validated a series of novel drug-like nanomolar NNMT inhibitors. Importantly, these drug candidates showed attractive cellular permeability flux when tested in membrane transport assays. Synthesis scale-up of the most promising drug candidates has been achieved. Proof-of-concept evaluations of individual drug candidates in mouse models of diet-induced obesity are awaiting final compound-specific IACUC approval, but are anticipated to commence within the month.

2. Keywords

metabolic disease

obesity and obesity-linked comorbidities

osteoarthritis

drug candidates

3. Accomplishments

Major goals of the project

Task 1: *In vitro* testing of *in silico* hits

1.1. Complete project hiring

Research scientists hired February 1, 2016 and February 15, 2016. Research technician hired August 8, 2016.

1.2. Order 70 small molecules for testing

Small molecules with good Vina “docking” (or virtual screening) scores were ordered for testing. To date, ~40-50 commercially available compounds have been testing in NNMT inhibition assays (see Figure 1). Based on initial results, novel analogs of a promising scaffold hit were evaluated using virtual screening protocols, and ~20-30 best scoring compounds synthesized and tested in NNMT inhibition assays. Drug-like nanomolar small molecule inhibitors of NNMT have been validated (see Table 1-5; please consider as confidential). Tested compounds have been analyzed and 2-dimensional and 3-dimensional structure-activity relationships have been established.

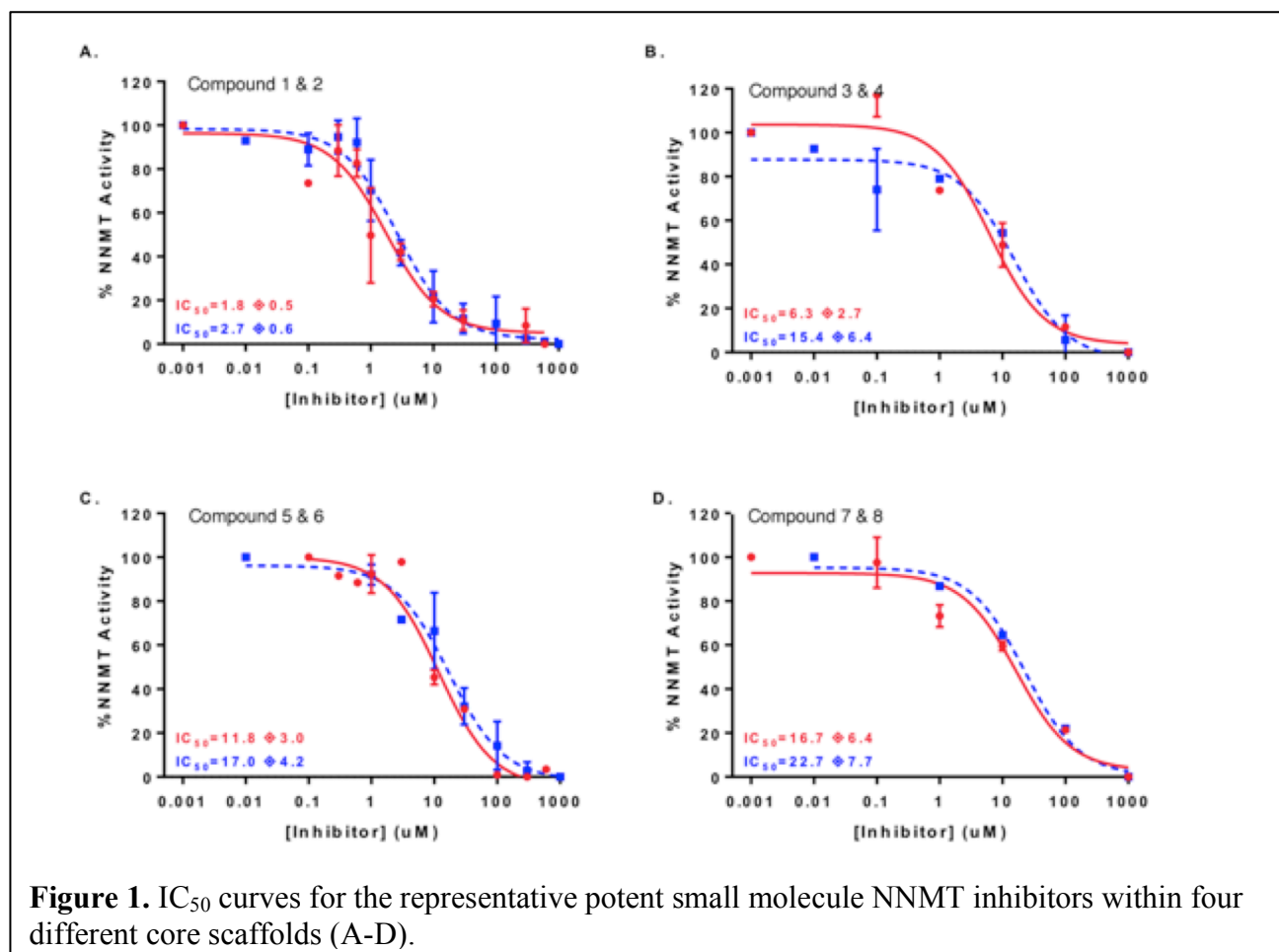
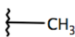
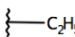
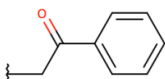
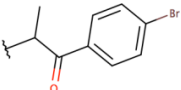
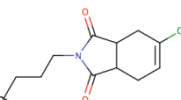
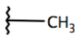
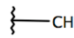
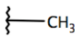

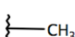

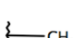
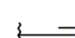

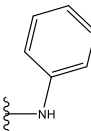
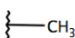
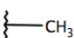
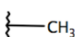
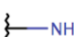


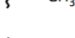

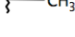

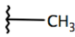
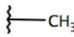










Table 1. NNMT inhibitory activity of scaffold A compounds with single positional substitutions

Compound Name	R1	R2	R3	R4	R5	R6	R7	R8	IC ₅₀ ± S.E. (uM)
1a		H	H	H	H	H	H	H	12.1 ± 3.1
1b		H	H	H	H	H	H	H	27.5 ± 4.4
1c	Methoxy-ethyl	H	H	H	H	H	H	H	165.1 ± 298
1d		H	H	H	H	H	H	H	>1000
1e		H	H	H	H	H	H	H	>1000
1f		H	H	H	H	H	H	H	>1000
1g			H	H	H	H	H	H	16.5 15.3 *
1h			H	H	H	H	H	H	6.3 ± 1.1
1i		H		H	H	H	H	H	2.6 ± 0.6
1j		H		H	H	H	H	H	23.8 ± 5.6
1k		H		H	H	H	H	H	>1000
1l		H	H		H	H	H	H	7.5 ± 2.2
1m		H	H		H	H	H	H	11.3 ± 11.7(R)
1n		H	H	H		H	H	H	0.9 ± 0.3
1o		H	H	H	H		H	H	5.7 ± 1.8
1p		H	H	H	H		H	H	13.1 ± 5.1
1q		H	H	H	H		H	H	52.4 ± 31
1r		H	H	H	H		H	H	468 ± 309?
1s		H	H	H	H	H		H	2.0 ± 0.5
1t		H	H	H	H	H		H	709 +/- 179 680?
1u		H	H	H	H	H	H		1.8 ± 0.5

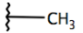
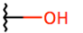
1v		H	H	H	H	H	H		48.7 ± 19.3
-----------	---	---	---	---	---	---	---	---	-----------------

Table 2. NNMT inhibitory activity of scaffold A compounds with dual positional substitutions

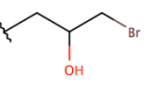
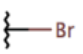
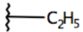
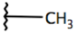
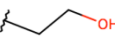
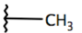
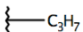
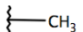
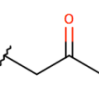
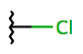
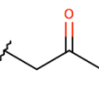
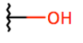
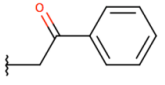
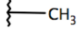
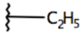
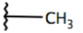
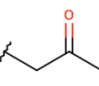
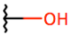

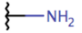


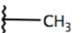


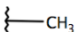
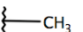
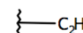
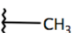
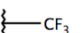


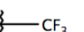

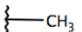
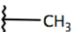
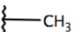
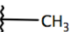
Compound Name	R1	R2	R3	R4	R5	R6	R7	R8	IC ₅₀ ± S.E. (uM)
2a		H		H	H	H	H	H	>1000
2b		H	H		H	H	H	H	9.8 ± 5.2
2c		H	H		H	H	H	H	33.5 ± 9.9
2d		H	H	H	H		H	H	>1000
2e		H	H	H	H		H	H	>1000
2f		H	H	H	H		H	H	>1000
2g		H	H	H	H		H	H	NI
2h		H	H	H	H	H	H		3.1 ± 1.4
2i		H	H	H	H	H	H		40.6 ± 13

Table 3. NNMT inhibitory activity of scaffold A compounds with multi-positional substitutions

Compound Name	R1	R2	R3	R4	R5	R6	R7	R8	IC ₅₀ ± S.E. (uM)
3a		H		H	H		H	H	1.1
3b		H	H		H		H	H	3.6 ± 1.5
3c			H	H	H		H	H	>1000
3d		H	H		H		H	H	>1000
3e		H	H		H	H	H		>1000??
3f			H		H		H		>1000

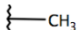
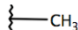
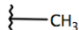
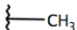
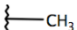
3g			H		H	H			>1000
-----------	---	---	---	---	---	---	---	---	-------

Table 4. NNMT inhibitory activity of compounds containing scaffold B

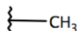
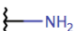
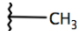
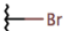
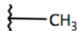
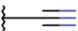
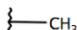
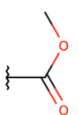
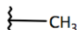
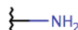
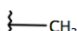

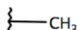
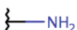
Compound Name	R1	R2	R3	R4	R5	R6	R7	R8	IC ₅₀ ± S.E. (uM)
4b	H			H	H	H	H	H	6.3 ± 2.7
4c	H		H		H	H	H	H	29.4 ± 6.4
4d	H		H		H	H	H	H	201.5 ± 204
4e	H		H		H	H	H	H	NI??
4f	H		H	H	H		H	H	29.9 ± 9.1
4g	H		H	H	H		H	H	>1000??
4h	H		H	H	H	H		H	>1000??

Table 5. NNMT inhibitory activity of compounds containing scaffold C

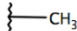
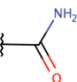
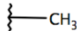
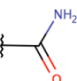
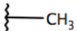
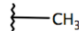
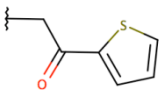
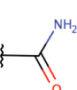
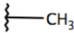
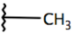
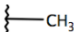
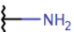
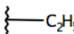
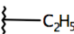
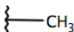
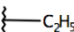
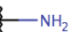
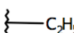
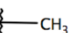
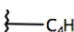
Compound Name	R1	R3	R4	R6	IC ₅₀ ± S.E. (uM)
5a			H	H	16.7 ± 3.8
5b					11.8 ± 3.0
5c			H	H	>1000

Table 6. NNMT inhibitory activity of compounds containing scaffold D.

Core/ Compound Name	R1	R3	R6	R7	X	IC ₅₀ ± S.E. (uM)
6a			H	H	N	16.7 ± 6.4
6b			H	H	N	82.4 ± 17.4
6c			H	H	N	22.7 ± 7.7
6d				H	N	>1000
6e		-		H	S	>1000
6f		-	H	H	S	>1000

1.3. Complete turbidity measurements in physiological buffer to determine solubility limits
Completed for each tested molecule.

1.4. Complete methyltransferase kinetic assay on initial set of soluble compounds
As noted under item 1.2, NNMT inhibition assays have been completed for 60+ compounds. Drug-like nanomolar small molecule inhibitors of NNMT have been validated. Tested compounds have been analyzed and 2-dimensional and 3-dimensional structure-activity relationships have been established. This process is continuing as we utilize existing data and improved predictive algorithms to design more effective small molecule inhibitors.

Milestone: Identify small molecule(s) NNMT inhibitor for subsequent cell culture study.

Achieved - small molecules for use as potential NNMT inhibitors in cell culture studies were proposed in November 2015. Following additional testing and validation, additional small molecule NNMT inhibitors were proposed in May, 2016 for testing in cell culture. The list of validated small molecule NNMT inhibitors appropriate for efficacy testing in adipocyte cell culture system is undergoing continual refinement as new compounds are tested.

1.5. Complete cell culture studies of 10 top-ranked compounds
Approximately 4 compounds have been tested to determine their effect on oxygen consumption in adipocyte cell culture. These studies used the Oxygraph system to measure oxygen flux, and collected data have suggested the tested compounds produce a phenotypic effect. We have recently developed a LC/MS assay to directly measure NNMT activity in cultured adipocytes; once fully characterized, this assay will be used to characterize the mechanistic activity of NNMT inhibitors in cell culture.

1.6. Complete metabolic stability of 5 top-ranked compounds
In progress, ~30% accomplished. Initial compounds were tested for metabolic stability using human and mouse microsomes. Studies were performed by Cyprotex (Watertown, MA), a valued Contract Research Organization, and completed December 3, 2015. We are currently refining our list of the most promising small molecule NNMT inhibitors for use in additional metabolic stability studies using Cyprotex.

1.7. Complete cytochrome P450 inhibition studies of 5 top-ranked cmpds
In progress, ~20% accomplished. We are currently refining our list of the most promising small molecule NNMT inhibitors for use in cytochrome P450 inhibition studies.

Task 2: *In vivo* testing of *in silico* hits

2.1. Local IRB/IACUC approval
IACUC protocol approval for treatment studies in diet-induced obesity (DIO) mouse models was obtained May 15, 2016. IACUC approval is required for each additional unique small molecule used to treat DIO mice. Currently, our local IACUC committee is reviewing ~6 small molecules planned for treatment studies in DIO mice.

Milestone: ACURO approval

Achieved – ACURO approval received on October 9, 2015.

2.2. Complete PK study of 4 top-ranked compounds

Pharmacokinetic (PK) studies of small molecule compounds completed on December 3, 2015 and August 8, 2016 using the Cyprotex (Watertown, MA), a valued Contract Research Organization. PK studies were performed in triplicate using mice, with compounds administered by subcutaneous injection. Plasma samples were collected at 7 time points over a 24 hr period. Test compounds were quantified by LC/MS and the time-dependent data used to calculate PK parameters (e.g., half-life, C_{max}).

2.3. Complete NOAEL study of 4 top-ranked compounds

In progress, ~20% complete. Will be completed within the next 1-2 months, immediately prior to *in vivo* efficacy testing.

Milestone: Identify small molecule(s) NNMT inhibitor for subsequent *in vivo* obesity-reversal study.

Achieved – 2 novel small molecule validated NNMT inhibitors (~1-3 μM IC_{50}) have been selected for proof-of-concept *in vivo* efficacy studies in DIO mice. Studies are planned to commence the 2nd week of January 2017, following a 1-month acclimation period for the subject animals. Each test compound has been synthesized in amounts > 1 g for use in these studies.

2.4. Complete diet-induced obesity-reversal study of 3 top-ranked compounds

In progress, ~ 25% complete. Approximately 20 DIO mice have been ordered and are expected to arrive early December. Animals will undergo a 1-month acclimation period. Studies are planned to commence the 2nd week of January 2017.

Milestone achieved: Complete proof-of-concept study to validate NNMT inhibitor as an anti-obesity lead.

In progress.

Task 3: Synthesis of novel transition-state (ts) analogs

3.1. Develop a multi-step synthesis of the novel transition-state inhibitor, which will be synthesized via a 9-step process based on some prior literature precedent.

A synthesis route has been designed, and we are currently troubleshooting the initial steps of this challenging reaction path.

3.2. Design and synthesis of 6 unique analogs of **SW-ts-0001**
Delayed, but planned for next 3 months.

3.3. Design and synthesis of additional 6 unique analogs of **SW-ts-0001** 6-12
Delayed, but planned for the next 3 months.

Milestone: Complete *de novo* synthesis of **SW-ts-0001** and ts analogs.

In progress, ~25% complete.

Task 4: *In vitro* testing of novel transition-state (ts) analogs

4.1 Turbidity measurements of ts analogs in physiological buffer
Delayed, but planned for next 3 months.

- 4.2. Complete methyltransferase kinetic assays of ts analogs
Delayed, but planned for next 3 months.
- 4.3. Complete cell culture studies of ts analogs
Delayed, but planned for next 3-4 months.

Milestone: Identify ts analog NNMT inhibitor for s *in vivo* obesity-reversal study.
In progress, ~20% complete.

Task 5: *In vivo* testing of novel transition state analogs

- 5.1. Complete PK study of 2 top-ranked ts analogs
To be completed by month 18.
- 5.2. Complete NOAEL study of 2 top-ranked ts analogs
To be completed by month 18.
- 5.3. Complete diet-induced obesity-reversal study of top-ranked ts analog
To be completed by month 18.

Milestone: Complete proof-of-concept study to validate ts analog NNMT inhibitor as an anti-obesity lead.
In progress for target date of month 18.

What opportunities for training and professional development has the project provided?
Nothing to Report.

How were the results disseminated to communities of interest?
Manuscript submitted to *Biochemistry* (see Appendix) and a second manuscript in preparation for submission to *J. Medicinal Chemistry*.

What do you plan to do during the next reporting period to accomplish the goals?
The major task for the next reporting period is to complete the planned proof-of-concept efficacy study of NNMT inhibitors in a mouse model of diet-induced obesity.

4. Impact

What was the impact on the development of the principal discipline(s) of the project?

As part of our efforts to discovery novel NNMT inhibitors, we have developed the first assay to utilize fluorescence spectroscopy to directly monitor NNMT product formation and activity in real-time. This assay provides accurate kinetic data that can be used to understand the molecular mechanistic details of the NNMT reaction. We were able to definitively show that NNMT follows a random bi-reactant mechanism in which each substrate could independently bind to the NNMT apoenzyme; however, both substrates bound to the complementary binary complexes with significantly lower affinity relative to independent binding. This reaction mechanism implies either substrate-induced conformational changes or bi-reactant intermolecular interactions may stabilize substrate binding to the binary complex and formation of the ternary complex. Additionally, our novel assay offers a robust detection technology for use in SAM substrate competition assays for the discovery and development of inhibitors of the large class of medically relevant SAM-dependent methyltransferases. As such, this research is of interest to pharmaceutical and academic researchers involved in drug discovery and enzyme structure-function studies.

What was the impact on other disciplines?

Nothing to Report.

What was the impact on technology transfer?

Nothing to Report.

What was the impact on society beyond science and technology?

Nothing to Report.

5. Changes/Problems

Changes in approach and reasons for change

Nothing to Report.

Actual or anticipated problems or delays and actions or plans to resolve them

Our research team has focused its limited synthetic chemistry resources on efforts to rapidly capitalize on the discoveries that were rapidly made in Aim 1. As such, work on synthesizing transition-state analogs as NNMT inhibitors (Aim 2) has been slightly delayed. However, with the synthetic chemistry efforts required to complete Aim 1 now significantly completed, our chemists will focus on rapidly completing synthesis of Aim 2 transition-state analogs. Moreover, the expertise we have gained in Aim 1 from developing and executing NNMT biochemical and cellular assays is expected to enable characterization of Aim 2 compounds to proceed rapidly.

Changes that had a significant impact on expenditures

Nothing to Report.

Significant changes in use or care of human subjects, vertebrate animals, biohazards, and/or select agents

Nothing to Report.

Significant changes in use or care of human subjects

Not applicable.

Significant changes in use or care of vertebrate animals

Nothing to Report.

Significant changes in use of biohazards and/or select agents

Not applicable.

6. Products

Publications, conference papers, and presentations

A manuscript was been submitted to *Biochemistry* (see Appendix) and a second manuscript is in preparation for submission to *J. Medicinal Chemistry*.

Journal publications

Harshini Neelakantan, Virginia Vance, Hua-Yu Leo Wang, Stanton F. McHardy, and Stanley J. Watowich; Non-coupled fluorescent assay for direct real-time monitoring of nicotinamide N-methyltransferase activity; *Biochemistry*; under review; federal support acknowledged.

Books or other non-periodical, one-time publications

Nothing to Report.

Other publications, conference papers, and presentations

Nothing to Report.

Website(s) or other Internet site(s)

Nothing to Report.

Technologies or techniques

We have developed the first assay to utilize fluorescence spectroscopy to directly monitor NNMT product formation and activity in real-time. This assay provides accurate kinetic data that can be used to understand the molecular mechanistic details of the NNMT reaction. Additionally, our novel assay offers a robust detection technology for use in SAM substrate competition assays for the discovery and development of inhibitors of the large class of medically relevant SAM-dependent methyltransferases. As such, this research is of interest to pharmaceutical and academic researchers involved in drug discovery and enzyme structure-function studies. This information is being shared via a journal submission.

Inventions, patent applications, and/or licenses

An invention disclosure (“Small molecule inhibitors of nicotinamide N-methyltransferase [NNMT]”) has been filed with the University of Texas Medical Branch’s Office of Technology Transfer regarding the synthesis and activity of small molecule NNMT inhibitors. **This disclosure** describes novel small molecule chemical entities that are to be used to inhibit the enzymatic activity of human nicotinamide N-methyltransferase (NNMT; CAS registry # 9029-74-7; EC 2.1.1.1). NNMT has been implicated in a number of diseases, including osteoarthritis, metabolic disorders (including, but not limited to, abnormal BMI, obesity, type 2 diabetes), cardiovascular disease, cancer (including, but not limited to, colorectal, breast, kidney, digestive tract, prostate, esophageal, pancreatic, endometrial, thyroid, gallbladder), metastatic progression, Parkinson's disease, kidney disease, and other neurovascular-related (e.g., migraine) and neurological dysfunctions (e.g., epilepsy). The described small molecule chemical entities could be used to treat and/or prevent some or all NNMT-associated diseases and/or their progression. These entities would be administered to people who are at risk for developing or are afflicted with NNMT-associated diseases. Additionally, the disclosed (and chemically related)

entities maybe used to facilitate weight loss and/or limit weight gain. If this disclosure results in a patent application, appropriate and timely notification to the granting agency will be made.

Other Products

Nothing to Report.

7. Participants & Other Collaborating Organizations

What individuals have worked on the project?

Name:	Stanley Watowich
Project Role:	PI
Researcher Identifier (e.g. ORCID ID):	ORCID ID: 0000-0002-1660-1818
Nearest person month worked:	3
Contribution to Project:	Project coordination and director; data analysis; computational SAR; assay design and development; inhibitor design
Funding Support:	DoD and UTMB
Name:	Stanton McHardy
Project Role:	PI of subcontract to University of Texas San Antonio
Researcher Identifier (e.g. ORCID ID):	
Nearest person month worked:	1
Contribution to Project:	Supervises all aspects of chemical synthesis related to this project
Funding Support:	UTSA
Name:	Harshini Neelakantan
Project Role:	Research scientist
Researcher Identifier (e.g. ORCID ID):	
Nearest person month worked:	12
Contribution to Project:	Designs, develops, optimizes, and performs biochemical and cell-based assays, and animal studies
Funding Support:	
Name:	Hua-Yu Wang
Project Role:	Research scientist
Researcher Identifier (e.g. ORCID ID):	
Nearest person month worked:	3
Contribution to Project:	Performs chemical synthesis of novel inhibitors; quality control and validation of commercial reagents
Funding Support:	UTSA
Name:	Virginia Vance

Project Role:	Research technician
Researcher Identifier (e.g. ORCID ID):	
Nearest person month worked:	4
Contribution to Project:	Optimizes and performs biochemical and cell-based assays
Funding Support:	

Has there been a change in the active other support of the PD/PI(s) or senior/key personnel since the last reporting period?

Nothing to Report.

What other organizations were involved as partners?

Nothing to Report.

8. Special Reporting Requirements

9. Appendices

Submitted manuscript attached.

This document is confidential and is proprietary to the American Chemical Society and its authors. Do not copy or disclose without written permission. If you have received this item in error, notify the sender and delete all copies.

Non-coupled Fluorescent Assay for Direct Real-time Monitoring of Nicotinamide N-Methyltransferase Activity

Journal:	<i>Biochemistry</i>
Manuscript ID	Draft
Manuscript Type:	Accelerated Publication
Date Submitted by the Author:	n/a
Complete List of Authors:	Neelakantan, Harshini ; University of Texas Medical Branch at Galveston, Biochemistry and Molecular Biology\ Vance, Virginia; University of Texas Medical Branch, Dept. of Biochemistry & Molecular Biology Wang, Hua-Yu; University of Texas San Antonio, Chemistry McHardy, Stanton; University of Texas San Antonio, Chemistry Watowich, Stanley; University of Texas Medical Branch, Dept. of Biochemistry & Molecular Biology

SCHOLARONE™
Manuscripts

Non-coupled Fluorescent Assay for Direct Real-time Monitoring of Nicotinamide N-Methyltransferase Activity

Harshini Neelakantan,[†] Virginia Vance,[†] Hua-Yu Leo Wang,[‡] Stanton F. McHardy,[‡] and Stanley J. Watowich^{†,*}

[†]Department of Biochemistry and Molecular Biology, University of Texas Medical Branch, Galveston, TX 77005 United States

[‡]Center for Innovative Drug Discovery, Department of Chemistry, University of Texas San Antonio, □ San Antonio, TX 78249 United States

ABBREVIATIONS

DTT, dithiothertol; KAN, kanamycin; IPTG, isopropyl- β -D-1-thiogalactopyranoside; 1-MNA, 1-methylnicotinamide; MTs, methyltransferases; 1-MQ, 1-methylquinolinium; NA, nicotinamide; NAD⁺, nicotinamide adenine dinucleotide; NNMT, nicotinamide *N*-methyltransferase; PMSF, phenylmethysulfonyl fluoride; Q, quinoline; SAH, *S*-5'-adenosyl-homocysteine; SAM, *S*-5'-adenosyl-L- methionine.

ABSTRACT: Nicotinamide N-methyltransferase (NNMT), an enzyme that catalyzes the transfer of a labile methyl group from the ubiquitous co-factor *S*-5'-adenosyl-L-methionine (SAM) to nicotinamide, pyridine, and structurally analogous compounds to form methylated end-products, has been implicated in metabolic disorders, cardiovascular disease, cancer, osteoarthritis, kidney disease, and Parkinson's disease. We have developed a novel non-coupled fluorescence-based methyltransferase assay that enables direct ultrasensitive real-time detection of the NNMT reaction product 1-methylquinolinium. This is the first assay reported to date to utilize fluorescence spectroscopy to directly monitor NNMT product formation and activity in real-time. This assay provided accurate kinetic data that enabled detailed comparative analysis of the NNMT reaction mechanism and kinetic parameters. A reaction model based on a random bi-reactant mechanism produced global curve fits that were most consistent with steady-state initial velocity data collected across an array of substrate concentrations. Based on the reaction mechanism, each substrate could independently bind to the NNMT apoenzyme; however, both substrates bound to the complementary binary complexes with ~20-fold lower affinity relative to independent binding. This reaction mechanism implies either substrate-induced conformational changes or bi-reactant intermolecular interactions may stabilize substrate binding to the binary complex and formation of the ternary complex. Importantly, this assay could rapidly generate concentration response curves for known NNMT inhibitors, suggesting its applicability for high-throughput screening (HTS) of chemical libraries to identify novel NNMT inhibitors. Furthermore, our novel assay offers a robust detection technology for use in SAM substrate competition assays for the discovery and development of SAM-dependent methyltransferase inhibitors.

Methyltransferases (MTs) are a broad family of enzymes that catalyze the methylation of various substrates, including proteins, nucleic acids (e.g., DNA, RNA), and endogenous small molecules (e.g., intracellular metabolites) using the co-factor *S*-5'-adenosyl-L-methionine (SAM) as a universal methyl donor.¹⁻⁷ Nicotinamide N-methyltransferase (NNMT) is an intracellular cytosolic small molecule methyltransferase enzyme that catalyzes the transfer of a labile methyl group from SAM to nicotinamide (NA), pyridine, and structurally analogous compounds, converting these substrates to *S*-5'-adenosyl-homocysteine (SAH), 1-methylnicotinamide (1-MNA), and other methylated end-products, respectively.^{8,9} Thus, NNMT directly regulates the detoxification of endogenous metabolites and exogenous xenobiotic products; intracellular levels of SAM and NA are regulated by NNMT contributing to the balance of metabolite turnover in the methionine-homocysteine cycle and the nicotinamide adenine dinucleotide (NAD⁺) synthesis pathways critical to cellular energy expenditure.¹⁰ Expression levels of NNMT are predominant and most well characterized in the liver;¹¹⁻¹³ however, NNMT is also present in the adipose tissue, kidney, brain, lung, heart, and muscle.^{8,14} There is a growing body of literature that corroborate an enhancement in NNMT expression and activity in a number of chronic disease conditions making it an interesting and viable therapeutic target for drug development.^{10,15-24} However, rapid discovery of NNMT-targeted small molecule inhibitors has been hampered by a lack of suitable real-time quantitative assays that can aid in the biochemical and kinetic characterization of both the enzyme activity and inhibitor's mechanism-of-action.

Existing NNMT assays monitor enzyme activity by direct or indirect detection of reaction products and the byproduct SAH such as the radiometric assay that utilizes ³H- and ¹³C-radiolabeled SAM to capture and directly quantify the transfer of the radiolabeled methyl group

to the substrates^{9, 12} or indirect chemical reaction-coupled fluorometric assays.^{9, 25} As reported in more recent studies, NNMT activity is monitored via measurement of absorbance of HPLC-separated reaction species,²⁶ independently or coupled to mass spectrometry.²⁷ Similar direct product detection methods (radiometric, radioisotope filter binding, scintillation proximity assay, anti-methylation antibody binding fluoroimmuno assays, and aptamer/riboswitch) and series of enzyme-coupled SAH detection colorimetric assays are used to probe the activity of many disease-linked MTs where the catalytic product readouts are single point, indirect, slow with multi-steps, labor intensive, and/or insensitive, and/or incorporate radioactive materials.²⁸⁻³⁷ These assays can be challenging and expensive to adapt for high throughput screening of large chemical libraries to identify MT inhibitors.³³

To date, there appears to be only one assay (for catechol-O-methyltransferase) described to directly detect methyltransferase product fluorescence,^{38, 39} and no current detection method provides direct, continuous, real-time, and sensitive monitoring of NNMT product formation. Herein, we describe a sensitive non-coupled fluorescence-based assay that monitors NNMT kinetic activity. Importantly, our fluorescent assay provides direct, continuous, and quantitative readout of the NNMT reaction, thus allowing detailed characterization of the NNMT reaction, inhibition constants, and inhibitor mechanism-of-action. To the best of our knowledge, this is the first assay that enables direct real-time spectroscopic monitoring of NNMT product formation that relies upon the NNMT selective substrate quinoline¹² that is methylated by SAM to form the product 1-methylquinolinium (1-MQ) with characteristic fluorescent properties. Direct real-time fluorescent readout of 1-MQ was used to define the NNMT reaction kinetic parameters (e.g., $K_{d,SAM}$, $K_{d,substrate}$, k_{cat}) and mechanism (e.g., product inhibition, sequential bimolecular binding,

random-order substrate binding) in contrast to most MT activity assays noted earlier where complete kinetic characterization has been rather challenging.³⁰

EXPERIMENTAL PROCEDURES

Chemicals and Reagents. Chemicals for the enzyme activity assays, including the co-substrates quinoline and SAM, the NNMT inhibitors 1-MNA and SAH, and 1-MQ for calibration curves were obtained from established commercial vendors. SAM, SAH, quinoline, and 1-MQ were obtained from Sigma Aldrich (St. Louis, MO) and 1-MNA chloride was obtained from the Cayman Chemical Company (Ann Arbor, MI). All compounds were reconstituted in double distilled water at the required concentrations. The identities of quinoline, 1-MQ, and 1-MNA were validated in house using NMR and mass spectroscopy, and purity for the compounds were confirmed to be >95% (conducted in the Center for Innovative Drug Discoveries at the University of Texas at San Antonio, TX).

Expression and Purification of Recombinant human NNMT. A codon-optimized plasmid (isopropyl- β -D-1-thiogalactopyranoside [IPTG]-inducible plasmid pJ401) corresponding to His-tagged human NNMT⁴⁰ was produced by DNA 2.0 (Menlo Park, CA). The recombinant human NNMT protein was expressed and purified to homogeneity by using protocols adapted and modified from Peng et al.⁴⁰ Briefly, the expression vector was used to transform chemically competent *E. coli* BL21 (DE3) cells. The BL21 transformants were plated on LB agar plate with kanamycin (KAN) (30 μ g/mL) and incubated overnight at 37°C that was used to inoculate 1L media along with 0.5 mM each of magnesium and calcium chloride for protein over-expression. The culture was placed in a shaker at 37°C to an OD₆₀₀ of 0.7-0.8 (~2-3 h) before induction with

0.5 mM IPTG and incubated for an additional 3 h. Cells were harvested by centrifugation at 10°C and 4000 rpm for 20 min and removal of the supernatant. For purification, harvested cells were first resuspended in chilled lysis buffer (20 mM Tris pH 7.9, 0.5 M NaCl, 5 mM imidazole, 10% glycerol, 1 mM DTT [dithiothertol], 1 mM PMSF [phenylmethylsulfonyl fluoride]) and the lysis mixture was sonicated on ice. Cell lysates were centrifuged at 4°C and 15000 rpm for 30 min. The soluble fraction was loaded onto a nickel affinity column formed from nickel sepharose beads (GE Biosciences) pre-equilibrated with lysis buffer. The column was washed with lysis buffer (5mM imidazole in lysis buffer) and increasing concentrations of NaCl (0.5 mM and 1 mM) followed by increasing concentrations of imidazole (5 mM and 20 mM, in lysis buffer) to remove contaminating proteins. Bound human NNMT was eluted from the column with lysis buffer and 150 mM imidazole, 200 mM salt, and 5% glycerol in 1 ml aliquots. Collected fractions were run on SDS-PAGE and Coomassie stained to verify purity and dialyzed into storage buffer (25 mM Tris, pH 8.6, 20% glycerol, 100 mM NaCl, 1 mM DTT). Pooled protein dialysate concentration was determined by UV spectroscopy, portioned into 100 uL aliquots (25 uM final stock concentration), flash-frozen in liquid nitrogen, and stored at -80°C for future use. Approximately 5 mg of purified NNMT was generated per liter of bacterial culture and the identity of the protein was confirmed by separating on SDS-PAGE followed by western blotting using an anti-NNMT primary antibody (ab119758; Abcam, 1:2000 dilution).

Steady-state Kinetic Assays for NNMT Activity. Reactions were performed at room temperature (25°C) in buffer consisting of 5 mM Tris pH 8.6 and 1 mM DTT. Immediately prior to initiating each set of reactions, freshly thawed NNMT was added to reaction buffers at a final concentration of 100 nM. Initial velocities were measured for independent reactions using

1
2
3
4
5
6
7
8
9
10
11
12
13
14
15
16
17
18
19
20
21
22
23
24
25
26
27
28
29
30
31
32
33
34
35
36
37
38
39
40
41
42
43
44
45
46
47
48
49
50
51
52
53
54
55
56
57
58
59
60

varying quinoline concentrations (25, 100, 200, 400, 600, 800 μ M) at different fixed concentrations of SAM (4, 8, 12, 20, 80, and 120 μ M). Separate reactions were performed in individual wells of a 96-well plate and all reactions were initiated by addition of SAM substrate. Since global fits of enzyme kinetic data can be sensitive to small differences in reaction concentrations, master stocks were used to minimize the number of titration steps required to prepare each individual reaction, thereby reducing potential differences in initial reaction concentrations due to pipetting errors. Following addition of NNMT and substrates, reaction progress was immediately monitored using a Micromax 96-well plate reader integrated into a double monochromator Fluorolog-3 spectrofluorometer (Horiba Jobin Yvon, Edison, NJ) and reaction data were collected approximately every minute for 10 minutes. The production of 1-MQ reaction product in each well was monitored by recording fluorescence emission intensities at 405 nm (excitation wavelength [λ_{ex}] 330 nm) with detector excitation and emission slit widths positioned at 4 nm. To compensate for potential fluctuations in instrument sensitivity between different experiments and across days, calibration curve data ([1-MQ] vs fluorescence intensity) were collected in parallel for each experiment and used to construct progress curves specific to each experiment.

NNMT Inhibition Assays. NNMT reactions were performed at room temperature in 96-well plates as described above, using reaction buffer containing 5 mM Tris pH 8.6, 1 mM DTT, and 10 μ M SAM. Immediately prior to initiating reactions, 100 nM of freshly-thawed NNMT was added and the reactions were initiated by adding 100 μ M quinoline substrate. Substrate concentrations were chosen such that they were substantially below the saturating concentrations that produced the maximum initial reaction velocity, yet were high enough to permit the non-

inhibited (control) reaction to produce 1-MQ significantly above background detection limits during the first 5 minutes of the reaction. Well studied MT/NNMT inhibitors SAM⁴¹ and 1-MNA⁸ were added as inhibitors to each reaction at half-log dilutions to generate concentration-response data that uniformly spanned a logarithmic scale. Fluorescence intensities were recorded, and data from the first 3 minutes (linear range of progress curves) of all reactions were used to calculate initial velocities at each inhibitor concentration.

Data Analysis. Fluorescence data obtained were transferred to GraphPad Prism (v7.0b; GraphPad Software, La Jolla, CA), which was used to perform linear regression analysis of replicate data to generate calibration curves and initial velocity measurements for all reactions. Initial velocities were measured for the linear portion of each reaction progress curve (initial 3-5 min) and under conditions where total product formed was less than <10% of the limiting substrate. The calculated steady-state initial velocity measurements and associated error estimates were used within the Prism software to generate individual Michaelis-Menten curves and kinetic parameters (i.e., $K_{m,substrate}$, V_{max}) for reaction datasets where one substrate concentration was fixed and the second substrate was varied as described above. The analysis of competing reaction models was performed using the DynaFit software package (BioKin, Watertown, MA). Each reaction model was automatically converted to a series of coupled ordinary differential equations (ODEs) under the assumption of rapid equilibrium, and nonlinear regression methods were used to calculate ODE parameters (corresponding to steady-state kinetic variables) that produced the best global fit of all kinetic data. Goodness-of-fit R^2 statistics provided a measure of the curve fit quality, and the computed Akaike Information Criteria was

used as the statistical measure to discriminate between competing models of the NNMT reaction mechanism.

Progress curve data (1-MQ fluorescent intensity vs time) for replicate dose response experiments (fixed substrate and enzyme concentrations, half-log dilutions of inhibitor concentration) for each inhibitor were transferred to the GraphPad Prism program and analyzed using the least-squares linear regression that was used to convert replicate kinetic data from the first 3 minutes of the reaction to initial velocity measurements. Initial velocities were then normalized (0-100%) and a single parameter (Hill slope = -1) dose response model (Normalized velocity = $100/(1+[\text{inhibitor}]/\text{IC}_{50})$) was fit to the data using least-squares nonlinear regression to calculate IC_{50} values and associated error estimates, and generate dose response curves.

RESULTS AND DISCUSSION

Protein Activity. Approximately 5 mg of purified NNMT were generated per liter of bacterial culture. Activity of newly purified protein was confirmed using well established and endogenous co-substrates, nicotinamide (NA; 100 μM final concentration) and S-adenosylmethione (SAM; 10 μM final concentration), and monitoring 1-methylnicotinamide (1-MNA) and S-adenosylhomocysteine (SAH) product formation in an HPLC-based absorbance assay as described previously.⁴⁰ Aliquots of NNMT stored at -80°C for at least 6 months did not show appreciable change in enzymatic activity relative to freshly purified protein (data not shown).

Fluorescent Assay Development. NNMT was observed to methylate several substrates analogous to pyridines including quinoline, similar to earlier reports.^{9, 27} 1-MQ was strongly

1
2
3
4
5
6
7
8
9
10
11
12
13
14
15
16
17
18
19
20
21
22
23
24
25
26
27
28
29
30
31
32
33
34
35
36
37
38
39
40
41
42
43
44
45
46
47
48
49
50
51
52
53
54
55
56
57
58
59
60

fluorescent with an emission maximum of 405 nm. The fluorescence excitation spectra ($\lambda_{\text{em}} = 405 \text{ nm}$) of quinoline (Q) and 1-MQ were appreciably different; 1-MQ showed a large excitation peak between 280-350 nm whereas quinoline showed little appreciable excitation at wavelengths longer than 320 nm (**Figure 1**). The differential excitation profile between 1-MQ and quinoline (**Table 1**) suggested that a spectrofluoroscopic approach might be used to directly observe NNMT reaction progress. The fluorescence intensity for 1-MQ at 405 nm showed ~25-fold greater intensity than quinoline, indicating fluorescent detection of the 1-MQ reaction product could be used to directly monitor NNMT activity. Importantly, in 96-well plates, the fluorescence signal ($\lambda_{\text{ex}} = 330 \text{ nm}$, $\lambda_{\text{em}} = 405 \text{ nm}$) of 1-MQ in NNMT reaction buffer was linearly correlated ($R^2 = 1$) with 1-MQ concentration over several orders of magnitude and with a detection limit of 100 nM in 5 mM Tris pH 8.6 reaction buffer (**Figure 2**). Figure 2 (insert) highlights the linear correlation between fluorescence signal and 1-MQ concentration over the concentration range most relevant to the measurement of initial product formation velocities for NNMT reactions. The 1-MQ detection limit could be lowered to ~40 nM when the reaction buffer contained 1 mM Tris (data not shown). Moreover, the slope of the 1-MQ calibration curve was essentially unchanged when 800 μM quinoline and/or 120 μM SAM were included in the reaction buffer.

The molecular mechanism and the values of the kinetic parameters associated with the NNMT reaction can be determined from accurate initial rate enzyme kinetics measured at varied SAM and quinoline substrate concentrations, with the assumption that the reaction achieves rapid substrate binding equilibrium. Progress curves of 1-MQ product formation as a function of time could be reproducibly measured from NNMT reactions performed in 96-well plates. As expected for enzyme kinetic studies, the collected progress curves were hyperbolic, with an

initial rapid linear reaction rate ($[1\text{-MQ}] \text{ s}^{-1}$) followed by progressively slower reaction rates until the 1-MQ concentration plateaued. The enzyme concentration in the NNMT reaction was adjusted to enable multiple fluorescent measurements to be simultaneously recorded from several dozen reaction wells during the initial linear velocity phase of the reaction. Using 100 nM concentration of NNMT for the kinetic reactions, the velocities of product formation were highly linear during the first 3-5 minutes of the reaction for all tested SAM substrate concentrations (**Figure 3**). Moreover, most reactions converted $<1\%$ of the limiting substrate to product during the initial linear velocity phase, and even reactions using the lowest tested initial SAM concentrations converted less than 8% of the starting substrate to product during the initial linear velocity phase. Linear regression analysis of the time-dependent kinetic data was used to calculate initial reaction velocities for SAM substrate concentrations ranging from 4 to 120 μM and quinoline substrate concentrations ranging from 25 to 800 μM ; goodness-of-fit R^2 values for the linear regression analysis ranged from 0.93 for the lowest tested substrate concentrations ($[\text{SAM}] = 4 \text{ }\mu\text{M}$, $[\text{quinoline}] = 25 \text{ }\mu\text{M}$) to >0.99 for the majority of tested substrate concentrations. Over the tested concentration ranges, initial velocity measurements had error estimates of $\sim 10^{-5} \text{ }\mu\text{M s}^{-1}$. The relative error in the initial velocity measurements ranged from 0.3% to 19%, with lower relative errors associated with the higher initial velocities that occurred at high substrate concentrations. The average and median relative errors observed with several dozen velocity measurements were 4.8% and 4.0%, respectively.

NNMT Kinetic Assay and Reaction Mechanism. Initial velocities were measured for reaction conditions with fixed NNMT concentration and a comprehensive matrix of substrate concentrations (SAM concentrations of 4, 8, 12, 20, 80, and 120 μM ; quinoline concentrations of 25, 100, 200, 400, 600, 800 μM). Initial velocity datasets consisting of a single SAM

concentration and a range of quinoline concentrations were plotted in conventional Michaelis-Menten format (initial velocity of 1-MQ product formation vs [Q]) and independent 2-parameter steady-state Michaelis-Menten curves ($v_o = v_{\max,app} [Q] / (K_{m,app} + [Q])$) were fit to each dataset with goodness-of-fit $R^2 > 0.98$ (**Figure 4A**). Similarly, the collected data could be transposed and individual steady-state Michaelis-Menten curves could be accurately fit to datasets consisting of a fixed quinoline concentration and a range of SAM concentrations. All curves asymptotically approached a maximum initial velocity at high substrate concentration, with no apparent substrate inhibition⁴² observed over the tested reaction conditions. The lack of observed substrate inhibition is in contrast to results reported using HPLC-MS to separate and characterize the NNMT reaction products.²⁷

Historically, steady-state kinetic studies of two substrate (or bi-reactant) enzymes have been analyzed using reciprocal plots (e.g., Lineweaver-Burk⁴³) that linearized the Michaelis-Menten equation (see Segel⁴⁴ and references therein). This approach was popularized by Cleland^{45, 46} as providing a graphical diagnostic to discriminate between conventional “ping-pong” and “sequential” reaction mechanisms that could be reduced to a closed-form analytical solution. Following this historical convention, initial velocity datasets consisting of a single SAM concentration and a range of quinoline concentrations were converted to double-reciprocal plots (**Figure 4B**), where each dataset fit to a linear equation with high accuracy (linear regression $R^2 > 0.99$). The lines corresponding to constant SAM concentrations in the double-reciprocal plot intersect at a single point, indicating a bi-reactant (also termed sequential) reaction mechanism in which NNMT forms a ternary complex with SAM and quinoline substrates, followed by the methyl transfer reaction that forms a transient complex of NNMT and the SAH and 1-MQ products. Since the constant SAM datasets did not form a series of parallel

lines in the double reciprocal plot, it is unlikely that NNMT operates via a “ping-pong” reaction mechanism.

The use of reciprocal plots to analyze bi-reactant kinetic data has largely been superseded by more accurate and robust nonlinear regression methods that calculate kinetic parameters by fitting ordinary differential equations corresponding to potential reaction mechanisms to all available initial velocity data.⁴⁷⁻⁴⁹ Moreover, modern global fitting methods can provide a rigorous statistical basis to discriminate between alternative reaction mechanisms (e.g., random bi-reactant, ordered bi-reactant).^{50, 51} A number of NNMT bi-reactant molecular models were constructed and simultaneously fit to all kinetic data using nonlinear regression analysis with a rapid-equilibrium approximation (**Table 2**). Akaike model discrimination, performed within the Dynafit suite, consistently selected a random bi-reactant reaction model with non-equivalent binding constants (**Figure 4C, D**) as the model that provided the best fit of the initial velocity data. In this comparative analysis, competing models (listed in **Table 2**) that did not provide good global fits of the initial velocity data included ordered bi-reactant models (also termed ordered sequential models) where either SAM (**Figure 4E, F**) or quinoline were required to first bind NNMT and random bi-reactant models with constant substrate binding constants (e.g., $K_{d,Q} = K_{d2,Q}$, $K_{d,SAM} = K_{d2,SAM}$).

It is interesting to note that the non-optimal model termed “random bi-reactant with constant $K_{d,substrate}$ ” produced binding constants ($K_{d,Q} = K_{d2,Q} = 92.2$ uM, $K_{d,SAM} = K_{d2,SAM} = 5.7$ uM; **Table 2**) that were largely equivalent to the K_m parameters ($K_{m,NA} = 105$ uM, $K_{m,SAM} = 5$ uM) determined in earlier enzyme kinetic studies⁴⁰ with an equivalent NNMT construct (triple-mutant hNNMT) and NA and SAM substrates. However, the rigorous kinetic analysis performed in our current study suggested that this model did not provide the best global fit of our extensive

set of initial velocity data, and thus its associated kinetic parameters likely do not accurately reflect details of the NNMT molecular mechanism. Instead, the NNMT mechanism was best described as a random bi-reactant reaction model with non-equivalent binding constants (**Table 2, Figure 4C, D**). This model, which is likely generally applicable for all NNMT xenobiotic reactants, implies that SAM or quinoline can initially bind to the NNMT apoenzyme, although the quinoline binding constant is ~20-fold higher than the SAM binding constant. Both SAM and quinoline have an ~20-fold improved binding affinity for the binary complex compared to the apoenzyme, suggesting that either (1) the binding of the first substrate perturbs the adjacent second substrate binding site to make it more favorable for coreactant binding or (2) the first bound substrate provides favorable intermolecular interactions of 7.4 kJ mol^{-1} ($1.77 \text{ kcal mol}^{-1}$) that stabilize the binding of the second substrate.

The kinetic parameters for the random bi-reactant reaction model with non-equivalent binding constants (reaction scheme, **Figure 4D**) could be refined to produce a slightly improved fit to the kinetic data by accounting for potential differences in NNMT concentrations in the different reaction datasets that might arise from small titration errors. Treating the NNMT concentration as a potentially adjustable parameter between independent reactions did not change the reaction model that was selected as producing the best fit of the kinetic data; however, adjusting by ~5% the enzyme concentration associated with two SAM datasets ([SAM] = 80 μM and 20 μM) produced an optimal global curve fits of the kinetic data as judged by Akaike weights and sum-of-squares statistics (**Table 2, Figure 4C**). The accuracy of the optimal global curve fits were essentially identical to the curve fits generated when Michaelis-Menten equations were independently fit to each separate dataset (compare **Figures 4A and 4C**); however, the global fits required fewer parameters and resulted in single values for all kinetic

parameters. Moreover, the kinetic parameters calculated for these optimal global curve fits and the global fits calculated when the NNMT concentration was not treated as an adjustable parameter (compare “random bi-reactant” and “random bi-reactant fixed [NNMT]” models in **Table 2**) were within the calculated error of each other.

When evaluating enzyme catalytic mechanisms, it is important to remember that a detailed analysis of kinetic data can identify models that are consistent with, or at odds with, experimental data. Such analysis can eliminate a proposed reaction model from consideration as responsible for an enzyme’s mechanism of action, but, as noted in studies dating back to Lineweaver and Burk,⁴³ this analysis cannot prove that a particular model correctly describes the enzyme’s reaction mechanism. The random bi-reactant reaction model with non-equivalent binding constants is most consistent with all currently available initial velocity data, although this model may require modification as additional experimental data are collected. For example, the random bi-reactant reaction model assumes NNMT, substrate-NNMT binary species, and the ternary complex satisfy a closed thermodynamic cycle with equilibrium binding constants linked as $K_{d,Q} K_{d2,SAM} = K_{d,SAM} K_{d2,Q}$ (reaction scheme, **Figure 4D**). However, nonlinear regression analysis of initial velocity kinetic data with a steady-state approximation cannot discriminate between models where a slow rate constant for the binding step essentially prevents the formation of one of the steady-state species. For example, a random bi-reactant reaction model that proposes quinoline binding to the NNMT*SAM binary complex is a kinetically disallowed event (reaction scheme, **Figure 4G**) that would fit the initial velocity data in the exact same manner as the random bi-reactant reaction model shown in Figure 4D. This is an intriguing model, since molecular docking studies predict that quinoline (and all NNMT xenobiotic substrates) would bind NNMT in a similar orientation as nicotinamide (**Figure 5A**) with the N1

atom of the methyl accepting substrate directed towards the reactive methyl moiety of SAM. In this orientation, quinoline is positioned at the terminus of a narrow closed tunnel that holds both SAM and the xenobiotic substrate (**Figure 5B**). SAM binding to the NNMT apoenzyme could effectively occlude this tunnel and conceivably prevent (or dramatically slow) quinoline from reaching its binding site. Subsequent studies will further refine the molecular binding events and rate constants associated with the NNMT reaction mechanism.

Inhibition Studies. The described real-time direct NNMT fluorescent assay can be utilized for robust high-throughput screening to identify small molecule inhibitors of NNMT and any SAM-dependent methyltransferase. In addition, this assay can facilitate detailed characterization of NNMT inhibitors, either through rigorous kinetic inhibition studies to determine an inhibitor's mechanism of action and binding affinity (K_i) or via IC_{50} studies to rapidly establish a compound's relative inhibitory potential. These applications will be expanded upon in future studies. However, as proof-of-concept, we completed IC_{50} studies to determine if NNMT reaction products could function as inhibitors (**Figure 6**). These studies serve as a foundation for developing small molecule NNMT inhibitors and for investigating product inhibition as a component of the NNMT reaction mechanism. Both SAH and 1-MNA (the presumed major physiological NNMT reaction product) strongly inhibited NNMT, with IC_{50} values of $5.5 \pm 0.5 \mu M$ and $9.0 \pm 0.6 \mu M$, respectively, calculated from dose response curves. The IC_{50} (SAH) value determined in this assay was comparable to the low micromolar value recently reported by van Harren,²⁷ although an IC_{50} value of 1-MNA was not reported. Importantly, in our fluorescent assay, the data of measured NNMT initial velocity vs [inhibitor] could be accurately fit ($R^2 = 0.98$) by a standard dose response inhibition curve (Hill slope = -1)

that displayed well-defined plateaus at both high and low inhibitor concentrations. These fits generated highly reproducible IC₅₀ measurements with errors of <10%. The low micromolar inhibitory activity determined for SAH and 1-MNA suggests that physiological concentrations of NNMT reaction products may modulate *in vivo* NNMT activity.

CONCLUSION

We describe a rapid, direct, ultrasensitive, convenient, cost-effective, non-coupled, and real-time analytical assay to monitor NNMT activity based on the fluorescence properties of a NNMT reaction product. This assay can generate accurate steady-state and pre-steady-state kinetic data that helps delineate the detailed reaction mechanism and kinetic parameters associated with NNMT-mediated catalysis. As demonstrated in our current studies, NNMT appears to operate through a random bi-reactant reaction mechanism, where each substrate can independently bind the apoenzyme. Significantly, the kinetic data enable detailed analysis that further showed both substrates bound their complementary binary complexes with ~20-fold lower affinity relative to binding the apoenzyme. Future broad-ranging kinetic studies with this assay will greatly facilitate mechanistic understanding of NNMT and related methyltransferases. Importantly, this assay can be directly used for the discovery, development, and characterization of NNMT inhibitors with the potential to fully understand mechanism of action and inhibition constants via detailed kinetic inhibition studies. Further, this assay is broadly applicable to any SAM-dependent methyltransferase, and can anchor a platform technology that utilizes SAM substrate competition to permit the discovery and development of SAM-dependent MT inhibitors. Given the expanding role of NNMT and other methyltransferases as molecular targets to develop therapeutics to combat numerous diseases, our robust 96-well plate format fluorescence-based

1
2
3
4
5
6
7
8
9
10
11
12
13
14
15
16
17
18
19
20
21
22
23
24
25
26
27
28
29
30
31
32
33
34
35
36
37
38
39
40
41
42
43
44
45
46
47
48
49
50
51
52
53
54
55
56
57
58
59
60

assay can be further miniaturized for efficient and effective high-throughput screening and will likely be of great utility for academic and pharmaceutical researchers.

ACKNOWLEDGEMENTS

We thank Drs. J. Lee and C. Finnerty for helpful discussions and Dr. P. Kuzmic for developing the Dynafit program and making it freely available for use.

AUTHOR INFORMATION

Corresponding Author

*Phone: (409) 747-4749. Email: watowich@xray.utmb.edu.

Funding

This work was supported by Department of Defense Peer Reviewed Medical Research Program grant PR141776 (S.J.W.) and a University of Texas Medical Branch Technology Commercialization Award (S.J.W.).

REFERENCES

[1] Syed, S. K., Kim, S., and Paik, W. K. (1993) Comparative studies on S-adenosyl-L-methionine binding sites of protein N-methyltransferases, using 8-azido-S-adenosyl-L-methionine as photoaffinity probe, *J Protein Chem* 12, 603-612.

[2] Martin, J. L., and McMillan, F. M. (2002) SAM (dependent) I AM: the S-adenosylmethionine-dependent methyltransferase fold, *Curr Opin Struct Biol* 12, 783-793.

[3] Zhang, X., and Cheng, X. (2006) Structure of protein arginine methyltransferases, *Enzymes* 24, 105-121.

[4] Copeland, R. A., Solomon, M. E., and Richon, V. M. (2009) Protein methyltransferases as a target class for drug discovery, *Nat Rev Drug Discov* 8, 724-732.

[5] Schapira, M., and Ferreira de Freitas, R. (2014) Structural biology and chemistry of protein arginine methyltransferases, *Medchemcomm* 5, 1779-1788.

[6] Kaniskan, H. U., Konze, K. D., and Jin, J. (2015) Selective inhibitors of protein methyltransferases, *J Med Chem* 58, 1596-1629.

[7] Hu, H., Qian, K., Ho, M. C., and Zheng, Y. G. (2016) Small Molecule Inhibitors of Protein Arginine Methyltransferases, *Expert Opin Investig Drugs* 25, 335-358.

[8] Aksoy, S., Szumlanski, C. L., and Weinshilboum, R. M. (1994) Human liver nicotinamide N-methyltransferase. cDNA cloning, expression, and biochemical characterization, *J Biol Chem* 269, 14835-14840.

[9] Alston, T. A., and Abeles, R. H. (1988) Substrate specificity of nicotinamide methyltransferase isolated from porcine liver, *Arch Biochem Biophys* 260, 601-608.

[10] Kraus, D., Yang, Q., Kong, D., Banks, A. S., Zhang, L., Rodgers, J. T., Pirinen, E., Pulinilkunnil, T. C., Gong, F., Wang, Y. C., Cen, Y., Sauve, A. A., Asara, J. M., Peroni, O. D., Monia, B. P., Bhanot, S., Alhonen, L., Puigserver, P., and Kahn, B. B. (2014) Nicotinamide N-methyltransferase knockdown protects against diet-induced obesity, *Nature* 508, 258-262.

[11] Cantoni, G. L. (1951) Methylation of nicotinamide with soluble enzyme system from rat liver, *J Biol Chem* 189, 203-216.

- [12] Rini, J., Szumlanski, C., Guercioli, R., and Weinshilboum, R. M. (1990) Human liver nicotinamide N-methyltransferase: ion-pairing radiochemical assay, biochemical properties and individual variation, *Clin Chim Acta* 186, 359-374.
- [13] Yan, L., Otterness, D. M., Craddock, T. L., and Weinshilboum, R. M. (1997) Mouse liver nicotinamide N-methyltransferase: cDNA cloning, expression, and nucleotide sequence polymorphisms, *Biochem Pharmacol* 54, 1139-1149.
- [14] Riederer, M., Erwa, W., Zimmermann, R., Frank, S., and Zechner, R. (2009) Adipose tissue as a source of nicotinamide N-methyltransferase and homocysteine, *Atherosclerosis* 204, 412-417.
- [15] Giulianti, R., Sartini, D., Bacchetti, T., Rocchetti, R., Kloting, I., Polidori, C., Ferretti, G., and Emanuelli, M. (2015) Potential involvement of nicotinamide N-methyltransferase in the pathogenesis of metabolic syndrome, *Metab Syndr Relat Disord* 13, 165-170.
- [16] Kannt, A., Pfenninger, A., Teichert, L., Tonjes, A., Dietrich, A., Schon, M. R., Kloting, N., and Bluher, M. (2015) Association of nicotinamide-N-methyltransferase mRNA expression in human adipose tissue and the plasma concentration of its product, 1-methylnicotinamide, with insulin resistance, *Diabetologia* 58, 799-808.
- [17] Parsons, R. B., Smith, M. L., Williams, A. C., Waring, R. H., and Ramsden, D. B. (2002) Expression of nicotinamide N-methyltransferase (E.C. 2.1.1.1) in the Parkinsonian brain, *J Neuropathol Exp Neurol* 61, 111-124.
- [18] Roessler, M., Rollinger, W., Palme, S., Hagmann, M. L., Berndt, P., Engel, A. M., Schneidinger, B., Pfeffer, M., Andres, H., Karl, J., Bodenmuller, H., Ruschoff, J., Henkel, T., Rohr, G., Rossol, S., Rosch, W., Langen, H., Zolg, W., and Tacke, M. (2005) Identification of nicotinamide N-methyltransferase as a novel serum tumor marker for colorectal cancer, *Clin Cancer Res* 11, 6550-6557.
- [19] Salek, R. M., Maguire, M. L., Bentley, E., Rubtsov, D. V., Hough, T., Cheeseman, M., Nunez, D., Sweatman, B. C., Haselden, J. N., Cox, R. D., Connor, S. C., and Griffin, J. L. (2007) A metabolomic comparison of urinary changes in type 2 diabetes in mouse, rat, and human, *Physiol Genomics* 29, 99-108.
- [20] Sartini, D., Muzzonigro, G., Milanese, G., Pierella, F., Rossi, V., and Emanuelli, M. (2006) Identification of nicotinamide N-methyltransferase as a novel tumor marker for renal clear cell carcinoma, *J Urol* 176, 2248-2254.

[21] Sartini, D., Santarelli, A., Rossi, V., Goteri, G., Rubini, C., Ciavarella, D., Lo Muzio, L., and Emanuelli, M. (2007) Nicotinamide N-methyltransferase upregulation inversely correlates with lymph node metastasis in oral squamous cell carcinoma, *Mol Med* 13, 415-421.

[22] Tomida, M., Mikami, I., Takeuchi, S., Nishimura, H., and Akiyama, H. (2009) Serum levels of nicotinamide N-methyltransferase in patients with lung cancer, *J Cancer Res Clin Oncol* 135, 1223-1229.

[23] Williams, A. C., and Ramsden, D. B. (2005) Autotoxicity, methylation and a road to the prevention of Parkinson's disease, *J Clin Neurosci* 12, 6-11.

[24] Xu, J., Moatamed, F., Caldwell, J. S., Walker, J. R., Kraiem, Z., Taki, K., Brent, G. A., and Hershman, J. M. (2003) Enhanced expression of nicotinamide N-methyltransferase in human papillary thyroid carcinoma cells, *J Clin Endocrinol Metab* 88, 4990-4996.

[25] Sano, A., Endo, N., and Takitani, S. (1992) Fluorometric assay of rat tissue N-methyltransferases with nicotinamide and four isomeric methylnicotinamides, *Chem Pharm Bull (Tokyo)* 40, 153-156.

[26] Patel, M., Vasaya, M. M., Asker, D., and Parsons, R. B. (2013) HPLC-UV method for measuring nicotinamide N-methyltransferase activity in biological samples: evidence for substrate inhibition kinetics, *J Chromatogr B Analyt Technol Biomed Life Sci* 921-922, 87-95.

[27] van Haren, M. J., Sastre Torano, J., Sartini, D., Emanuelli, M., Parsons, R. B., and Martin, N. I. (2016) A Rapid and Efficient Assay for the Characterization of Substrates and Inhibitors of Nicotinamide N-Methyltransferase, *Biochemistry* 55, 5307-5315.

[28] Barrow, E. W., Clinkenbeard, P. A., Duncan-Decocq, R. A., Perteet, R. F., Hill, K. D., Bourne, P. C., Valderas, M. W., Bourne, C. R., Clarkson, N. L., Clinkenbeard, K. D., and Barrow, W. W. (2012) High-throughput screening of a diversity collection using biodefense category A and B priority pathogens, *J Biomol Screen* 17, 946-956.

[29] Drake, K. M., Watson, V. G., Kisielewski, A., Glynn, R., and Napper, A. D. (2014) A sensitive luminescent assay for the histone methyltransferase NSD1 and other SAM-dependent enzymes, *Assay Drug Dev Technol* 12, 258-271.

[30] Duchin, S., Vershinin, Z., Levy, D., and Aharoni, A. (2015) A continuous kinetic assay for protein and DNA methyltransferase enzymatic activities, *Epigenetics Chromatin* 8, 56.

- [31] Jurkowska, R. Z., Ceccaldi, A., Zhang, Y., Arimondo, P. B., and Jeltsch, A. (2011) DNA methyltransferase assays, *Methods Mol Biol* 791, 157-177.
- [32] Kumar, S., King, L. E., Clark, T. H., and Gorovits, B. (2015) Antibody-drug conjugates nonclinical support: from early to late nonclinical bioanalysis using ligand-binding assays, *Bioanalysis* 7, 1605-1617.
- [33] Luo, M. (2012) Current chemical biology approaches to interrogate protein methyltransferases, *ACS Chem Biol* 7, 443-463.
- [34] Rye, P. T., Frick, L. E., Ozbal, C. C., and Lamarr, W. A. (2011) Advances in label-free screening approaches for studying histone acetyltransferases, *J Biomol Screen* 16, 1186-1195.
- [35] Su, Y., Hickey, S. F., Keyser, S. G., and Hammond, M. C. (2016) In Vitro and In Vivo Enzyme Activity Screening via RNA-Based Fluorescent Biosensors for S-Adenosyl-l-homocysteine (SAH), *J Am Chem Soc* 138, 7040-7047.
- [36] Wood, R. J., McKelvie, J. C., Maynard-Smith, M. D., and Roach, P. L. (2010) A real-time assay for CpG-specific cytosine-C5 methyltransferase activity, *Nucleic Acids Res* 38, e107.
- [37] Wu, Q., Gee, C. L., Lin, F., Tyndall, J. D., Martin, J. L., Grunewald, G. L., and McLeish, M. J. (2005) Structural, mutagenic, and kinetic analysis of the binding of substrates and inhibitors of human phenylethanolamine N-methyltransferase, *J Med Chem* 48, 7243-7252.
- [38] Barrow, J. C. (2012) Inhibitors of Catechol-O-Methyltransferase, *CNS Neurol Disord Drug Targets* 11, 324-332.
- [39] Kimos, M., Burton, M., Urbain, D., Caudron, D., Martini, M., Famelart, M., Gillard, M., Barrow, J., and Wood, M. (2016) Development of an HTRF Assay for the Detection and Characterization of Inhibitors of Catechol-O-Methyltransferase, *J Biomol Screen* 21, 490-495.
- [40] Peng, Y., Sartini, D., Pozzi, V., Wilk, D., Emanuelli, M., and Yee, V. C. (2011) Structural basis of substrate recognition in human nicotinamide N-methyltransferase, *Biochemistry* 50, 7800-7808.

[41] Borchardt, R. T., Huber, J. A., and Wu, Y. S. (1974) Potential inhibitor of S-adenosylmethionine-dependent methyltransferases. 2. Modification of the base portion of S-adenosylhomocysteine, *J Med Chem* 17, 868-873.

[42] Tomlinson, S. M., and Watowich, S. J. (2008) Substrate inhibition kinetic model for West Nile virus NS2B-NS3 protease, *Biochemistry* 47, 11763-11770.

[43] Lineweaver, H., and Burk, D. (1934) The Determination of Enzyme Dissociation Constants, *Journal of the American Chemical Society* 56, 658-666.

[44] Segel, I. H. (1975) *Enzyme kinetics : behavior and analysis of rapid equilibrium and steady state enzyme systems*, Wiley, New York.

[45] Cook, P. F., and Cleland, W. W. (2007) *Enzyme kinetics and mechanism*, Garland Science, London ; New York.

[46] Morrison, J. F., and Cleland, W. W. (1980) A kinetic method for determining dissociation constants for metal complexes of adenosine 5'-triphosphate and adenosine 5'-diphosphate, *Biochemistry* 19, 3127-3131.

[47] Kuzmic, P. (1996) Program DYNAFIT for the analysis of enzyme kinetic data: application to HIV proteinase, *Anal Biochem* 237, 260-273.

[48] Kuzmic, P. (2006) A generalized numerical approach to rapid-equilibrium enzyme kinetics: application to 17beta-HSD, *Mol Cell Endocrinol* 248, 172-181.

[49] Kuzmic, P. (2009) DynaFit--a software package for enzymology, *Methods Enzymol* 467, 247-280.

[50] Collom, S. L., Laddusaw, R. M., Burch, A. M., Kuzmic, P., Perry, M. D., Jr., and Miller, G. P. (2008) CYP2E1 substrate inhibition. Mechanistic interpretation through an effector site for monocyclic compounds, *J Biol Chem* 283, 3487-3496.

[51] Kuzmic, P., Cregar, L., Millis, S. Z., and Goldman, M. (2006) Mixed-type noncompetitive inhibition of anthrax lethal factor protease by aminoglycosides, *FEBS J* 273, 3054-3062.

[52] Sanner, M. F. (1999) Python: a programming language for software integration and development, *J Mol Graph Model* 17, 57-61.

TABLES

Table 1. Relative Fluorescence of 1-Methylquinolinium (1-MQ) and Quinoline (Q).

Fluorescent intensity measurements were performed in 96-well plates using 10 uM solutions.

λ_{ex} (nm)	λ_{em} (nm)	$\text{FI}_{1\text{-MQ}} / \text{FI}_Q$
310	405	15
320	405	20
330	405	25
340	405	25

Table 2. Kinetic Parameters Derived for Competing NNMT Reaction Mechanisms

Mechanism	AIC*	K _{d,SAM} (uM)	K _{d,Q} (uM)	K _{d2,SAM} (uM)	K _{d2,Q} (uM)	k _{cat} (s ⁻¹)
Random bi-reactant	0.997	45.1 ± 8.8	842.0 ± 233.7	2.1 ± 0.4	39.2 ± 5.4	0.024 ± 0.0005
Random bi-reactant (fixed [NNMT])	0.003	39.9 ± 9.3	848.9 ± 299.0	2.0 ± 0.5	41.5 ± 6.7	0.023 ± 0.0005
Random bi-reactant with constant K _{d,substrate}	0.0	5.7 ± 0.6	92.2 ± 11.0	5.7 ± 0.6	92.2 ± 11.0	0.026 ± 0.001
Ordered (SAM first) bi-reactant	0.0	82.9 ± 18.8	-	-	27.3 ± 5.8	0.022 ± 0.0005
Ordered (Q first) bi-reactant	0.0	no convergence				

*Akaike Information Criteria

FIGURES and FIGURE LEGENDS

Figure 1. Comparative fluorescence excitation spectra for 10 μM solutions of 1-methylquinolinium (1-MQ, top curve) and quinoline (Q, bottom curve). Fluorescence emission intensities (counts s^{-1} ; cps) were recorded at $\lambda_{\text{em}} = 405 \text{ nm}$.

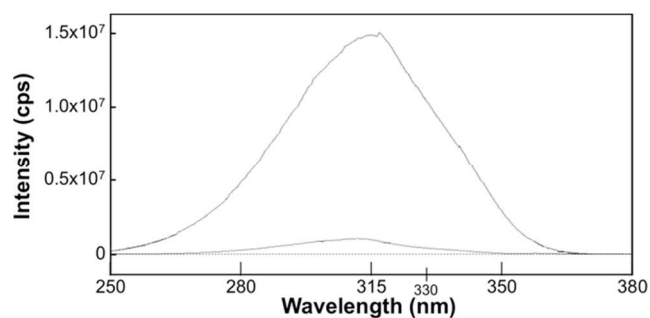


Figure 2. Representative calibration curve showing linear response ($R^2 = 1$) between 1-MQ concentrations and fluorescent signal ($\lambda_{\text{ex}} = 330 \text{ nm}$, $\lambda_{\text{em}} = 405 \text{ nm}$). Insert panel shows data points for the lower 1-MQ concentrations. Buffer conditions were 5 mM Tris pH 8.6, 1 mM DTT. Data points and errors bars (which in all cases are similar in size to the data point symbol) represent averages and standard deviations from 9 replicate experiments. Slope and y-intercept of displayed curve is 3642 ± 4.9 and 576 ± 46.7 , respectively.

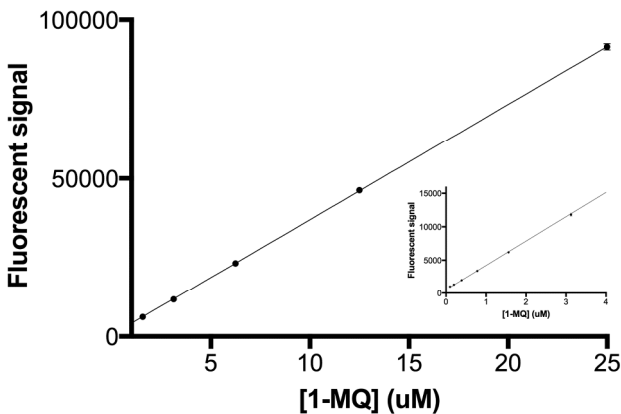


Figure 3. Real-time progress curves for representative NNMT reactions showing linear response data used to calculate initial reaction velocities (v_o). Fluorescent intensities ($\lambda_{\text{ex}} = 330$ nm, $\lambda_{\text{em}} = 405$ nm) from 1-MQ product generation were continuously recorded and converted to molar concentrations using simultaneously measured calibration curve data. For these representative reactions, assay conditions were 5 mM Tris pH 8.6, 1 mM DTT, 80 μ M SAM, and 100 nM NNMT, with quinoline concentrations ranging from 25 μ M to 800 μ M. Error bars represent standard deviations from 3 experiments. Linear regression analysis for the representative curves had goodness-of-fit $R^2 > 0.9988$.

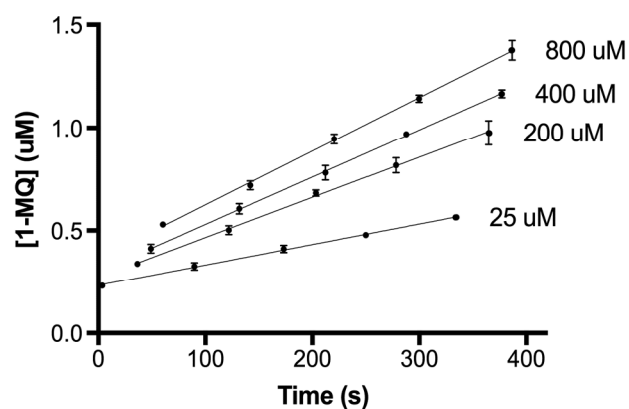
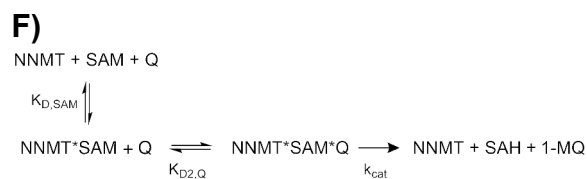
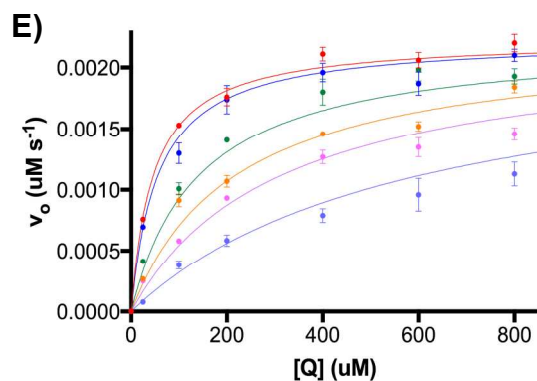
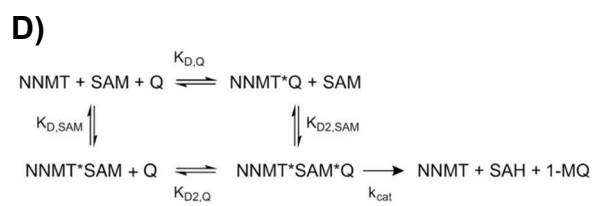
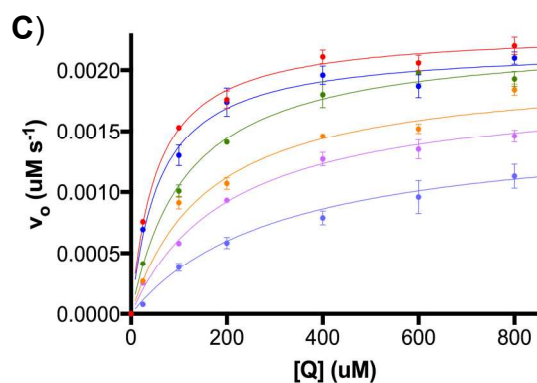
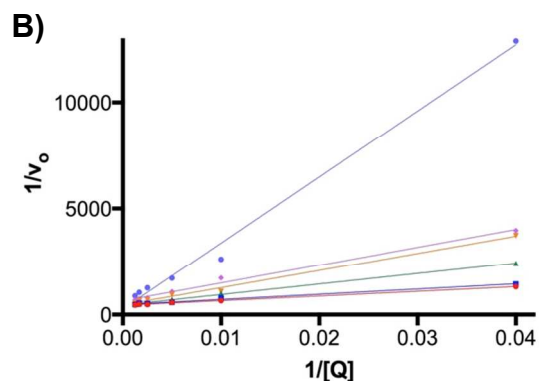
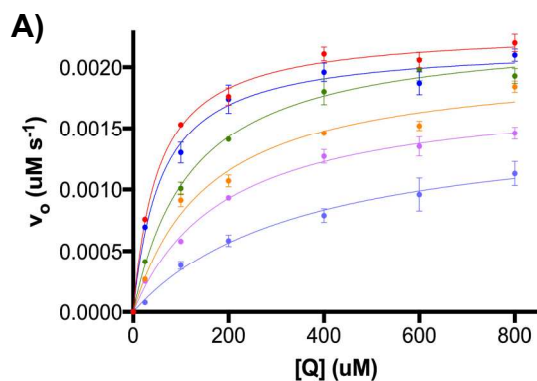


Figure 4. Michaelis-Menten plots for NNMT kinetic data. Datasets represent initial velocities (average value, $n=3$) measured over a range of quinoline concentrations and at fixed SAM concentrations. **A.** Datasets for reactions performed at several SAM concentrations were independently fit to single-substrate Michaelis-Menten curves ($v_o = v_{\max,app} [Q] / (K_{m,app} + [Q])$). Goodness-of-fit R^2 values were 0.996, 0.991, 0.997, 0.983, 0.997, and 0.994 for curves corresponding to $[SAM] = 120, 80, 20, 12, 8,$ and $4 \mu M$, respectively. **B.** Double reciprocal plot for kinetic reactions performed over a range of quinoline concentrations, where each line corresponds to a fixed SAM reaction concentration. Linear regression R^2 values were greater than 0.99 for all fitted lines. **C.** Global fit (nonlinear regression analysis sum of squares = 1.3×10^{-7}) of all kinetic data measurements using a random bi-reactant reaction mechanism. **D.** Schematic of the random bi-reactant reaction mechanism that produces the global curve fits shown in panel C. **E.** Optimal global fit (nonlinear regression analysis sum of squares = 3.2×10^{-7}) of all kinetic data using an ordered (SAM first) bi-reactant reaction mechanism. **F.** Schematic of the ordered (SAM first) bi-reactant reaction mechanism that produces the global curve fits shown in panel E. **G.** Schematic of a random bi-reactant reaction mechanism with a kinetically blocked binding step that would similarly produce the global curve fits shown in panel C. Curves in Figures A, B, C and E correspond to reactions with $[SAM] = 120 \mu M$ (red curve), $80 \mu M$ (blue curve), $20 \mu M$ (green curve), $12 \mu M$ (orange curve), $8 \mu M$ (magenta curve), and $4 \mu M$ (cyan curve). Error bars represent standard deviations ($n=3$). Chemical reaction schematics prepared with ChemDraw (v 13.0).



Ordered (SAM first) bi-reactant mechanism does not provide the best fit to kinetic data.

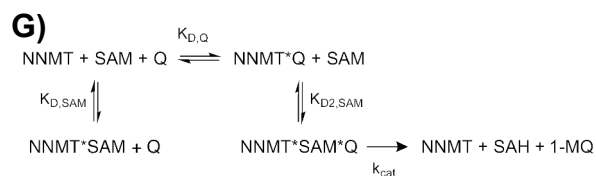


Figure 5. Model structure of quinoline substrate bound to the NNMT nicotinamide (NA) substrate binding site. (A) Ribbon representation of NNMT with NA (green molecule) and SAH (teal molecule) as bound in the X-ray cocrystal structure (PDB 3ROD⁴⁰). The bound conformation of quinoline (orange molecule) is predicted to overlap the NA substrate, with the methyl accepting nitrogen atoms positioned in essentially equivalent positions. (B) Surface representation for NNMT highlighting the deep internal cavity that encloses the NA, quinoline, and SAM binding sites. The arrow indicates where the internal cavity opens to the bulk solvent surrounding NNMT. Figures produced with AutoDock Tools.⁵²

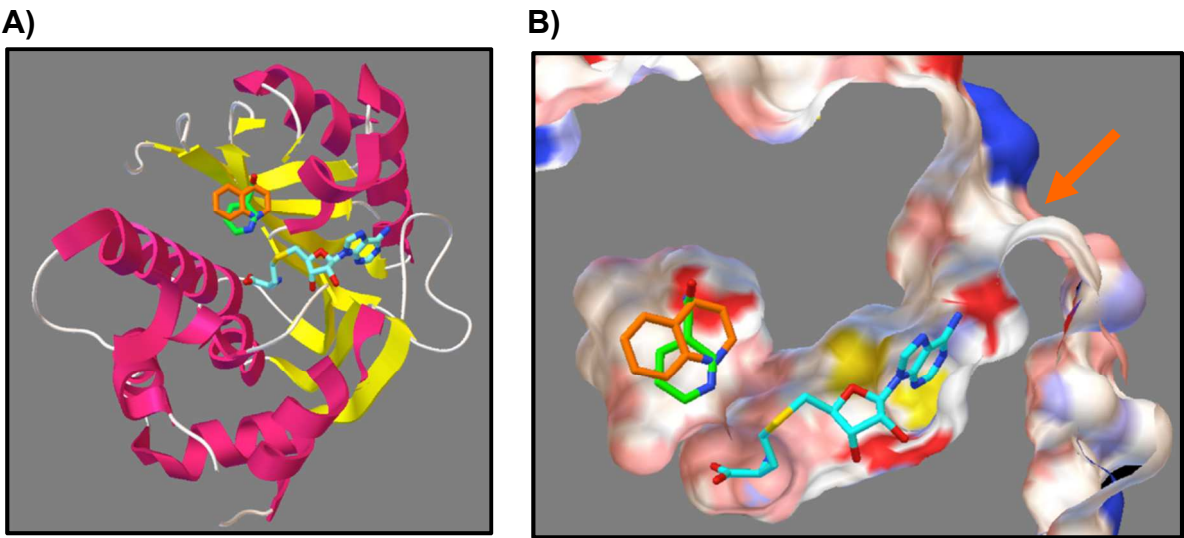
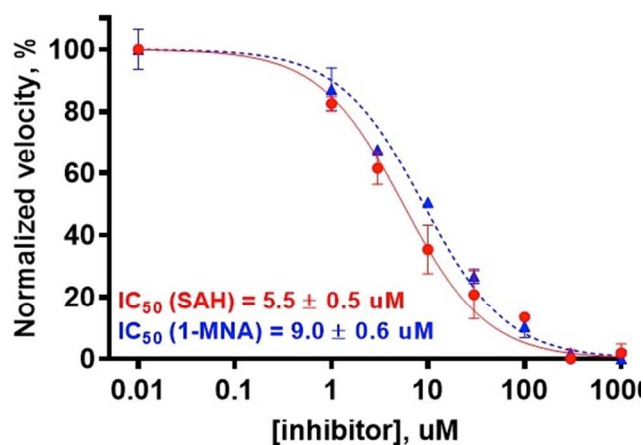


Figure 6. Normalized response curves (Hill slope = -1) for NNMT inhibitors (SAH, solid red curve; 1-MNA, dashed blue curve). Data points represent average and standard deviation of normalized initial reaction velocities measured from replicate (n=3) experiments. For both compounds, the goodness-of-fit R^2 between the fitted curves and data was 0.98.



GRAPHIC FOR TABLE OF CONTENTS

For Table of Contents Use Only: Non-coupled Fluorescent Assay for Direct Real-time Monitoring of Nicotinamide N-Methyltransferase Activity; Harshini Neelakantan, Virginia Vance, Hua-Yu Wang, Stanton F. McHardy, and Stanley J. Watowich

